Cognitive Deficits in Anti-LGI1 Encephalitis Are Linked to Immunotherapy-Resistant White Matter Network Changes

Stephan Krohn,[1,2,]* Leonie Müller-Jensen,[1,3,]* Joseph Kuchling,[1,3] Amy Romanello,[1,2] Katharina Wurdack,[1,4] Sophia Rekers,[1,2] Thorsten Bartsch,[5] Frank Leypoldt,[6,7] Friedemann Paul,[1,4,8,9] Christoph J. Ploner,[1] Harald Prüss,[1,10] and Carsten Finke[1,2]

Correspondence
Dr. Finke
carsten.finke@charite.de

Abstract

Background and Objectives

Cognitive deficits represent a major long-term complication of anti–leucine-rich, glioma-inactivated 1 encephalitis (LGI1-E). Although severely affecting patient outcomes, the structural brain changes underlying these deficits remain poorly understood. In this study, we hypothesized a link between white matter (WM) networks and cognitive outcomes in LGI1-E.

Methods

In this cross-sectional study, we combined clinical assessments, comprehensive neuropsychological testing, diffusion tensor MRI, probabilistic WM tractography, and computational network analysis in patients with LGI1-E referred to Charité-Universitätsmedizin Berlin. Healthy individuals were recruited as control participants and matched to patients for age and sex with logistic regression propensity scores.

Results

Twenty-five patients with LGI1-E (mean age = 63 ± 12 years, 76% male) and 25 healthy controls were enrolled. Eighty-eight percent of patients presented persistent cognitive symptoms at postacute follow-up (median: 12 months from onset, interquartile range: 6–23 months)—despite treatment with immunotherapy and good overall recovery (modified Rankin Scale [mRS] score at peak illness vs postacute: $z = -4.1$, $p < 0.001$, median mRS score at postacute visit: 1). Neuroimaging revealed that WM networks in LGI1-E are characterized by (1) a systematic reduction in whole-brain connectivity ($t = -2.16$, $p = 0.036$, $d = -0.61$), (2) a cortico-subcortical hypoconnectivity cluster affecting both limbic and extralimbic brain systems, and (3) a "topological reorganization" marked by a bidirectional shift in the relative importance of individual brain regions in the WM network. The extent of this WM reorganization was strongly associated with long-term deficits of verbal memory ($r = -0.56$), attention ($r = -0.55$), and executive functions ($r = -0.60$, all $p_{FDR} = 0.017$).

Discussion

Although traditionally viewed as a form of limbic encephalitis, our study characterizes LGI1-E as a "network disorder" that affects the whole brain. Structural reorganization of WM networks was linked to long-term and multidomain cognitive impairment, which was not prevented by immunotherapy. These findings highlight the need for closer monitoring and improved treatment strategies to mitigate long-term cognitive impairment in LGI1-E.

---

*These authors contributed equally to this work as co-first authors.

[1]Department of Neurology and Experimental Neurology, Charité - Universitätsmedizin Berlin, corporate member of Freie Universität Berlin and Humboldt- Universität zu Berlin; [2]Berlin School of Mind and Brain, Humboldt-Universität zu Berlin; [3]Berlin Institute of Health at Charité – Universitätsmedizin Berlin, BIH Charité Clinician Scientist Program; [4]NeuroCure Clinical Research Center, Berlin; [5]Department of Neurology, University Medical Center Schleswig-Holstein, Campus Kiel; [6]Department of Neurology, Christian-Albrecht University of Kiel and University Medical Center Schleswig-Holstein; [7]Neuroimmunology, Institute of Clinical Chemistry, Christian-Albrecht University of Kiel and University Medical Center Schleswig-Holstein; [8]ECRC Experimental and Clinical Research Center; [9]Max Delbrück Center for Molecular Medicine in the Helmholtz Association (MDC); and [10]German Center for Neurodegenerative Diseases (DZNE) Berlin, Berlin, Germany.

Glossary

Introduction

Anti–leucine-rich, glioma-inactivated 1 encephalitis (LGI1-E) represents the most common form of autoimmune encephalitis (AE) in older adults.[1] Caused by autoantibodies against the synaptic LGI1 antigen,[2] LGI1-E commonly presents with prodromal symptoms including the pathognomonic facio-brachial dystonic seizures that can precede other manifestations by weeks to months.[3-5] Subsequently, most patients develop a combination of memory impairment, temporal lobe seizures, sleep disturbances, confusion, and behavioral abnormalities[1,6]—a clinical syndrome conceptualized as "limbic encephalitis"[7] that is frequently accompanied by T2/FLAIR hyperintensities of the medial temporal lobe (MTL) in clinical MRI.[8,9]

More recently, however, advanced neuroimaging studies have increasingly suggested a key role of extralimbic brain systems in LGI1-E. Specifically, previous reports have demonstrated a widespread disruption of extralimbic functional networks, including the default mode, sensorimotor, salience, and higher visual network,[10,11] paralleled by metabolic abnormalities in the basal ganglia, motor areas, and prefrontal cortex.[12,13] Similarly, microstructural brain damage as assessed with diffusion-weighted imaging (DWI) has been observed in both limbic and extralimbic brain structures and correlates with poorer functional outcomes.[8,14]

In parallel, clinical studies have identified cognitive deficits as a crucial outcome of LGI1-E, showing that these deficits (1) persist for years after peak illness,[5,8] (2) represent a key predictor of long-term functional disability,[15] and (3) encompass diverse cognitive functions beyond a classical "limbic" syndrome, including executive functions, language skills, psychomotor speed, and attention.[10,16-18]

Given this combination of limbic and extralimbic manifestations, we hypothesized that—beyond focal damage to individual regions—LGI1-E may specifically affect the brain's white matter (WM) network that connects limbic and extralimbic brain systems. Therefore, we combined DWI-based probabilistic WM tractography,[19] graph-theoretical network analyses,[20] clinical evaluation, and comprehensive neuropsychological assessments to study the relationship between WM networks and cognitive outcomes in patients with LGI1-E.

Methods

Study Population

We prospectively enrolled 25 patients with LGI1-E referred to our reference center at the Department of Neurology at Charité-Universitätsmedizin Berlin, Germany, between January 2013 and April 2022. All patients fulfilled current diagnostic criteria[21] and tested positive for anti-LGI1 antibodies in serum and/or CSF with indirect immunofluorescence assays. MRI and neuropsychological testing were performed on referral. The median time from onset to study visit was 12 months (interquartile range [IQR], 6–23). In 6 patients, time from onset to referral was <6 months. MRI and cognitive testing were performed on the same day, except for 4 patients in whom MRI was conducted 2, 3, 4, and 6 months after neuropsychological testing, respectively. Clinical data were collected using standardized case report forms. The modified Rankin Scale (mRS) and the Clinical Assessment Scale in Autoimmune Encephalitis (CASE)[22] were scored retrospectively by 2 investigators (L.M.J. and K.W.). Partial data of 16 patients have been analyzed in previous work,[10] albeit regarding other imaging modalities. A diagnosis of depression and/or arterial hypertension at the time of MRI was assessed retrospectively through medical referral letters and patient reports for post hoc analysis of the WM findings.

As a control cohort, we included 25 healthy individuals who were matched to patients for age and sex using logistic regression propensity scores and nearest-neighbor matching, as implemented in the MatchIt package for R (version 3.0.2).[23]

Cognitive Assessment

Cognitive performance in patients with LGI1-E was assessed with standardized neuropsychological examination. Following previous approaches,[10] test performance was quantified with composite scores across 5 cognitive domains: (1) visuospatial memory (Rey-Osterrieth Complex Figure Test; immediate and delayed recall scores), (2) verbal episodic memory (German edition of the Rey Auditory Verbal Learning Test; supraspan, interference, and delayed recall scores), (3) attention (Test Battery for Attention Performance [TAP]; median reaction times and standard deviations for tonic and phasic alertness, and divided visual and auditory attention), (4) executive functions (TAP Go/NoGo median reaction time), and (5) working memory (forward and

backward digit span test scores). Composites were calculated by first z-scoring individual subscores and subsequently averaging over these z-scores within a cognitive domain, where reaction times were inverted to ensure that higher composite scores consistently indicate better performance across all cognitive domains. Moreover, for normative interpretation of cognitive performance, individual test scores were converted to percentile ranks using age-specific norms and labeled as "below-average performance" at values ≤16th percentile and "significant impairment" at ≤7th percentile, as detailed in the eMethods.

MRI Preprocessing and Connectome Construction

Brain MRI was performed at the Berlin Center for Advanced Neuroimaging using a 3T Tim Trio scanner (Siemens, Erlangen, Germany) with a 12-channel phased-array head coil. Details on image acquisition parameters can be found in the eMethods. DWI preprocessing and tractography were performed using MRtrix3,[24] FSL,[25] and ANTs[26] as described previously.[27] In brief, we performed denoising, eddy current correction, and motion correction for DWI sequences. To achieve global intensity normalization, we conducted bias field correction and DWI group normalization.

Anatomical T1-weighted scans were parcellated into 84 cortical and subcortical regions of interest (ROIs) using the Desikan-Killiany atlas (DKA)[28] and segmented into WM and gray matter (GM) using FSL-FAST.[29] Then, T1-weighted scans were registered to DWI scans, and using a group average response function for normalization, fiber orientation density functions were obtained using single-shell, single-tissue constrained spherical deconvolution. Anatomically constrained probabilistic tractography and spherical-deconvolution informed filtering of tractograms 2 (SIFT2) were conducted to create biologically accurate connectomes from 2×10^7 streamlines,[19,27,30] as recently validated in AE.[31] The output file was an 84×84 structural connectivity (SC) matrix, where each cell value represents the absolute streamline count of the respective ROI-to-ROI connection. To achieve interparticipant connection density normalization, each value of the matrix was multiplied by the participant-specific fiber density SIFT2 proportionality coefficient (μ), resulting in weighted and normalized SC matrices.

Region-to-Network Mapping

Assignment of anatomical regions to functional brain systems was implemented with a novel mapping algorithm. This procedure assigned each of the 84 ROIs in the DKA to one of the 7 canonical resting-state networks from the Multiresolution Intrinsic Segmentation Template,[32] which includes the cerebellum, mesolimbic network, somatomotor network, visual network, default mode network, frontoparietal/visual-downstream network, and ventral attention network/salience network/basal ganglia/thalamus as functional clusters. Further details on region-to-network mapping can be found in the eMethods.

Network Analysis and Graph-Theoretical Measures

White matter networks—commonly referred to as structural "connectomes"[33]—were analyzed with the custom code and the Brain Connectivity Toolbox.[34] Tractography yielded symmetrical connectome matrices, where the diagonal was set to 0 to discard self-connections. Furthermore, individual connectomes were normalized by the maximally observed connectivity, such that connection strengths were standardized to lie within $[0,1]$ for each participant. Subsequently, network sparsity was implemented by thresholding the connection strength and setting all elements below the threshold to 0, following common practice.[20] Therein, we applied a set of linearly increasing cutoff values from 0 to the 95th percentile by increments of 5, resulting in 20 thresholded connectomes of increasing sparsity for each participant. Because it is an open question which sparsity threshold is optimal for subsequent network analyses (and because this threshold is arbitrary by definition), we computed the area under the curve over all 20 thresholds, yielding a single summary measure.

At each threshold, connectomes were subjected to an analysis of network topology for weighted and undirected graphs, in which we estimated the node degree (ND) and betweenness centrality (BC) for every brain region. The mathematical formulation and conceptualization of these graph-theoretical measures for brain networks have been described in detail previously.[20,34,35] In brief, ND quantifies the number of structural links that pass through a given node, yielding a measure of its overall "connectedness." Note that ND values here were symmetrical because network graphs were undirected, such that the connectivity between region A → region B was identical to that of region B → region A. Moreover, BC values for weighted networks were calculated for every brain region. This measure expresses the proportion of all shortest paths in the network that pass through a given node, commonly interpreted to indicate its "hubness" (that is, its relative importance in the network), because it expresses the propensity of the node to exert a bridging role in the network.[20,34]

Topology Deviation Index

To quantify changes in the whole-brain topology of structural connectomes, we defined a topology deviation index (TDI), which rests on recent methodological developments[36] and was computed as follows: First, a reference topology was calculated over all healthy participants as the median BC value for each brain region, yielding a 1×84 vector of reference values for the DKA. In this study, we chose BC as the target graph metric because it expresses topological network organization rather than connectivity alone and because group analyses suggested widespread and bidirectional connectome reorganization in patients with LGI1-E. Subsequently, we related this reference distribution to the regional centrality values of individual participants. Topological deviation was then calculated as TDI = $1 - \rho_s$, i.e., the nonparametric correlation distance between the reference centrality values and

the individual centrality values, where ρ_s refers to the Spearman rank correlation coefficient. In this study, we chose rank-based over product-moment correlation because the former does not assume a linear relationship between the 2 variables and is less sensitive to outliers. The TDI thus resolves to 0 if an individual brain topology perfectly adheres to the reference topology in rank space and gradually increases to >0, the more the individual values deviate from this reference. Note that this approach thus captures topological network changes across all brain regions simultaneously, yielding a single whole-brain deviation value for each participant.

Statistical Analysis

Univariate between-group differences were assessed as the standardized effect size for independent-sample t tests (Cohen's d). The ordinal mRS and CASE scores were assessed once at peak illness and once at postacute follow-up, such that these samples were paired and assessed with the nonparametric signed-rank test. Continuous relationships were tested with product-moment correlation or rank-based correlation, as indicated. Differences in network topology between patients and controls were assessed with a permutation approach. The null hypothesis under this regime posits that there is no between-group difference and that, consequently, there is no effect of whether a particular participant is labeled a patient or a control. To test this hypothesis, one then estimates the null distribution of the statistic under question by randomly permuting the group labels and recalculating the statistic for every permutation. The ensuing p value of this test is then given as the number of instances in which the randomly permuted statistics surpass the value of the empirically observed statistic, divided by the total number of random permutations (here, n = 5,000). When a variable was repeatedly tested against multiple other measures, we applied the Benjamini-Hochberg procedure to control the false discovery rate (FDR).[37]

Standard Protocol Approvals, Registrations, and Participant Consents

All participants gave written informed consent. Our study followed the STROBE guidelines, was performed in accordance with the Declaration of Helsinki, and was approved by the ethics committee of Charité-Universitätsmedizin Berlin (EA4/011/19).

Data Availability

Data and analysis code to reproduce the findings of this study will be made available on the Open Science Framework (osf.io/uf29k/).

Results

Patient Characteristics

The study population included 25 patients with LGI1-E (6 women; mean age: 63 ± 12 years) and 25 healthy controls (HCs) (10 women; mean age: 59 ± 11 years) matched for age (t = 1.38, p = 0.175) and sex (χ^2 = 0.83, p = 0.363). All patients had received first-line immunotherapy (IV steroids, plasma exchange, IV immunoglobulins), and 68% underwent second-line immunotherapy (rituximab, azathioprine). Further clinical characteristics are summarized in Table 1.

Clinical and Cognitive Outcomes

First, we sought to characterize the clinical outcomes in our study cohort from peak illness to the postacute study visits at which the MRI recordings were acquired. Therefore, we analyzed clinical scores on the mRS and the more disease-specific CASE, as presented in Figure 1. Patients showed a reduction in mRS scores from peak to postacute follow-up (Figure 1A; z = −4.1, p < 0.001, n = 25), with 88% of patients presenting a postacute mRS score ≤2, commonly regarded as a "good" functional outcome.[38] Similarly, the CASE sum score across all clinical subdomains decreased markedly from peak to postacute follow-up (Figure 1B; z = −3.9, p < 0.001, n = 25). However, patient outcomes varied strongly across the CASE subdomains (Figure 1C, left), with memory dysfunction being the most prevalently affected domain at peak illness (96% of patients affected), followed by seizures (92%) and psychiatric symptoms (56%). It is important to note that only 12% of patients showed complete absence of memory symptoms at postacute follow-up while this was 48% for seizures and 64% for psychiatric symptoms (Figure 1C, right). Patients thus presented long-term cognitive symptoms despite good overall outcomes on standard clinical assessment scales.

To characterize the distribution of these symptoms across cognitive domains, we conducted a normative interpretation of the postacute neuropsychological scores, as summarized in Table 2. Using predefined cutoff values, we observed that 24 of 24 patients showed *below-average* performance in at least one cognitive test and 22 (92%) of 24 patients further showed *significant* impairment in at least one domain. Although all cognitive domains were affected, the highest impairment rates were observed for verbal episodic memory and attention.

SC Analysis

Regarding the tractography results, we first assessed whether patients with LGI1-E exhibit systematic differences in SC, as presented in Figure 2. To this end, we extracted the total number of estimated WM tracts for each participant to compare region-to-region SC (Figure 2A) and whole-brain SC (Figure 2B) between patients and HCs. Patients predominantly presented reduced SC among individual GM regions (Figure 2A) and showed lower whole-brain SC compared with HCs (Figure 2B; t = −2.16, p = 0.036, d = −0.61).

To assess the spatial distribution of these SC reductions, we subsequently thresholded the network-wide differences to p < 0.001 and observed the strongest effects in a spatial cluster of deep GM structures and neocortical areas (Figure 2C). Specifically, these connectivity reductions clustered in the hippocampus, caudate, accumbens, and thalamus and a variety of

Table 1 Clinical Characteristics of the Patient Sample

Characteristic	Patients, no. (%) LGI1-E (n = 25)
Symptoms during the acute disease stage	
Memory impairment	24/25 (96)
Psychiatric symptoms	14/25 (56)
Sleep disturbance	8/22 (36)
FBDS	12/25 (48)
Other seizures (including autonomic seizures)	16/25 (64)
SIADH/hyponatremia	13/25 (52)
Diagnostics	
MRI	
Any MRI abnormality[a]	19/24 (79)
Hippocampal T2/FLAIR hyperintensity/edema (bilaterally)	6/24 (25)
Hippocampal T2/FLAIR hyperintensity/edema (unilaterally)	5/24 (21)
Basal ganglia T2/FLAIR hyperintensity/edema	1/24 (4)
EEG abnormalities[b]	14/22 (64)
Comorbidity at MRI	
Diagnosed with depression	5/20 (25)
Diagnosed with arterial hypertension	7/19 (37)
Malignant disease	0/23 (0)
Treatment	
Days from onset to treatment, median (IQR)	48 (11–133)
Steroids (IV)	25/25 (100)
Plasma exchange	16/25 (64)
Intravenous immunoglobulins (IVIGs)	9/25 (36)
Rituximab	15/25 (60)
Azathioprine	5/25 (20)
Antipsychotic or antidepressant medication	3/25 (12)
Antiseizure medication	20/25 (80)
Months from onset to MRI, median (IQR)	12 (6–23)
Outcome	
mRS score at peak (median, range)	3 (2–4)
mRS score at MRI (median, range)	1 (0–3)
CASE score at peak (median, range)	4 (2–8)
CASE score at MRI (median, range)	2 (0–5)
Relapse	7/19 (37)
Fatal outcome	0/25 (0)

Abbreviations: CASE = Clinical Assessment Scale for Autoimmune Encephalitis; FBDS = faciobrachial dystonic seizures; FLAIR = fluid-attenuated inversion recovery; IVIGs = IV immunoglobulins; IQR = interquartile range; MTL = medial temporal lobe; mRS = modified Rankin Scale; SIADH = syndrome of inappropriate antidiuretic hormone secretion; WM = white matter.
[a] Includes MTL T2/FLAIR hyperintensity and edema, unilateral or bilateral hippocampal T2/FLAIR hyperintensity with or without gadolinium enhancement, global atrophy, MTL atrophy, WM lesions, and leukoencephalopathy.
[b] Includes diffuse slow activity, focal slow activity, and epileptic activity.

neocortical areas, most notably the caudal anterior cingulate, lateral occipital gyrus, the precentral and postcentral gyri, and the inferior parietal and superior frontal gyri (Figure 2D, left). Using a novel region-to-network mapping procedure (see Methods), we identified that these connectivity reductions clustered in the mesolimbic network—in line with the traditional conception of LGI1-E as a form of "limbic" encephalitis[7]—but additionally affected a wide range of extralimbic brain systems including attentional/salience, motor, visual, and default mode areas (Figure 2D, right).

Further supporting these findings, graph analysis of WM networks showed that LGI1-E is characterized by systematic decreases in ND—a measure that quantifies the overall connectedness of individual brain regions (see Methods). Here again, we found ND to be most strongly decreased in the hippocampus (left: $d = -1.16$, $p_{perm} < 0.001$; right: $d = -1.01$, $p_{perm} < 0.001$), but reductions were also observed across multiple subcortical and neocortical areas (Figure 2E, left). As for raw connectivity estimates, network mapping revealed widespread extralimbic ND reductions, most notably including default mode, frontoparietal, and attentional/salience areas (Figure 2E, right).

Network Topology Analysis

Next, we studied how LGI1-E affects the topological organization of WM networks beyond connectivity reductions. To this end, we applied a graph-theoretical framework and estimated the normalized BC for each GM region. In brief, BC measures the relative importance of a node in the network by quantifying the number of all shortest paths in the network that pass through it. In consequence, a brain region shows high BC if it lies on many shortest paths connecting other brain regions and thus exerts a "bridging role" in the network.[20] Notably, comparing BC values between patients with LGI1-E and HCs revealed that patients exhibit bidirectional changes in network centrality: Figure 3A shows that BC was *increased* in patients in the amygdala bilaterally (left: $d = 0.61$, $p_{perm} = 0.016$; right: $d = 0.72$, $p_{perm} = 0.006$) and across various neocortical regions (strongest effects: left inferior parietal cortex: $d = 0.63$, $p_{perm} = 0.010$; left parahippocampal gyrus: $d = 0.61$, $p_{perm} = 0.014$). These BC increases clustered in multiple brain areas beyond the limbic system, most prominently the frontoparietal network (Figure 3A, *right*).

Simultaneously, however, patients with LGI1-E also showed *decreased* BC across several other brain regions (Figure 3B). These centrality reductions clustered in deep GM areas and were strongest in the hippocampus (right: $d = -0.96$, $p_{perm} < 0.001$; left: $d = -0.84$, $p_{perm} = 0.002$), the right caudate nucleus ($d = -0.71$, $p_{perm} = 0.006$), and the left thalamus ($d = -0.78$, $p_{perm} = 0.005$). Here again, extralimbic brain systems were strongly affected, most notably subcortical and attentional/salience areas (Figure 3B, *right*).

In sum, patients with LGI1-E show a "topological reorganization" of WM networks, characterized by a bidirectional shift in the relative importance of individual brain regions in the network.

Figure 1 Patients With Anti-LGI1 Encephalitis Show Long-Term Cognitive Symptoms Despite Good Overall Recovery on Standard Clinical Assessment Scales
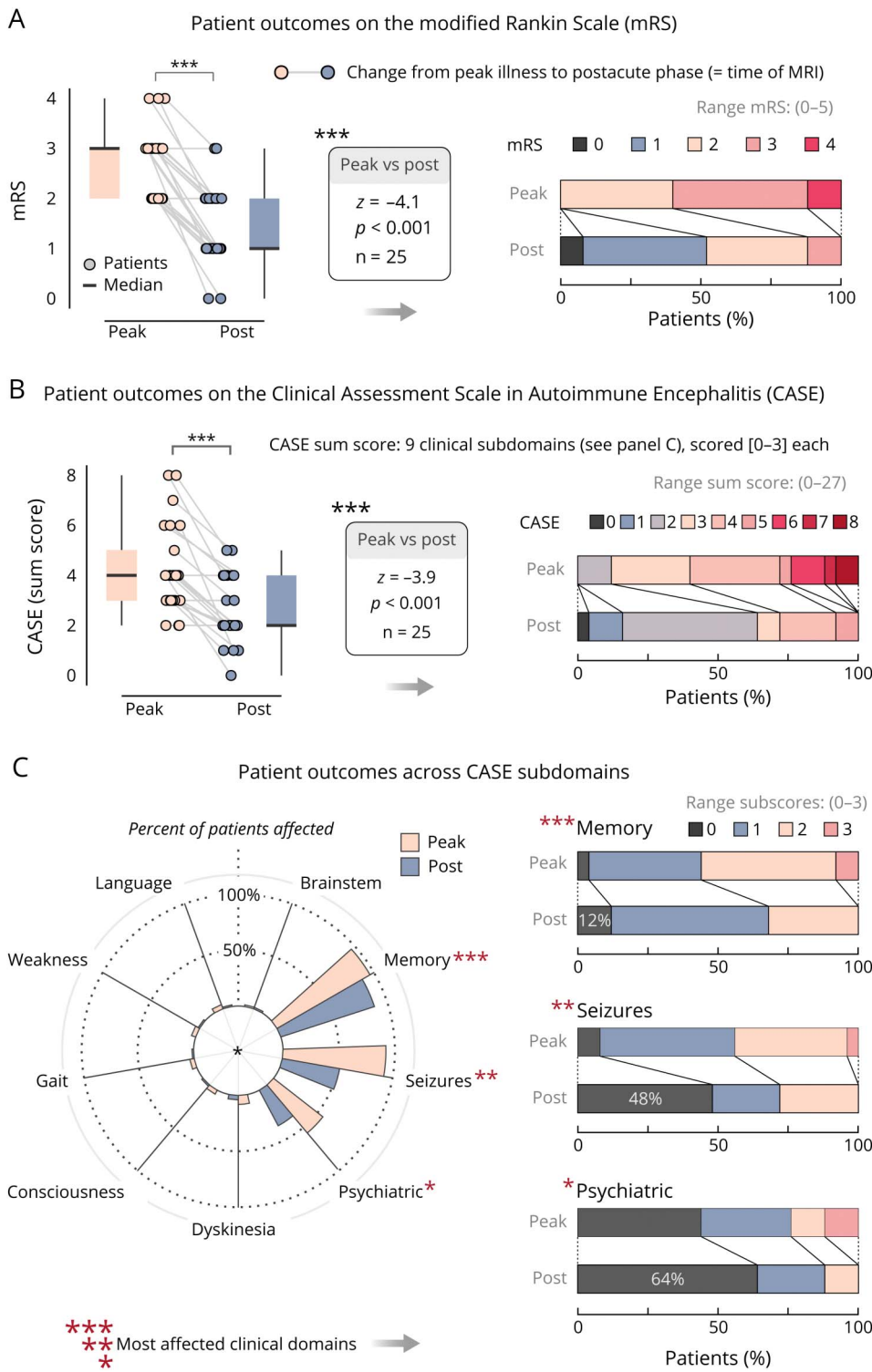
(A) Patient outcomes on the modified Rankin Scale (mRS) from peak illness to the postacute phase. MRI recordings underlying the imaging analyses were obtained at postacute follow-up. Peak vs postacute scores were compared with the Wilcoxon signed-rank test. (B) Patient outcomes on the Clinical Assessment Scale in Autoimmune Encephalitis (CASE). The CASE sum score is given by the sum over 9 clinical subdomains, each scored with [0–3]. (C) Patient outcomes across CASE subdomains. The polar plot shows the percentage of affected patients at peak illness and postacute follow-up. The bar plots relate patient outcomes across the 3 most prevalent clinical subdomains: memory dysfunction, seizures, and psychiatric symptoms.

WM Reorganization and Cognitive Outcomes

Given these neuroimaging findings, we finally focused on cognitive outcomes specifically and asked how the reorganization of WM networks relates to postacute cognitive performance in LGI1-E. To this end, we first computed a reference topology over all HC participants as the median BC for every brain region (Figure 4A). We then derived the novel *TDI* as the nonparametric correlation distance between this reference distribution in HCs and the corresponding centrality values of each individual participant (see Methods).

Table 2 Cognitive Performance of Patients With LGI1-E at Postacute Visit

	Raw score (mean ± SD)	No. of patients below average of reference	No. of patients with significant impairment
Visuospatial memory			
ROCF: immediate recall	17.5 ± 8.0	4/21 (19%)	3/21 (14%)
ROCF: delayed recall	16.4 ± 10.0	4/15 (27%)	4/15 (27%)
Verbal episodic memory			
RAVLT: supraspan	5.2 ± 1.6	9/22 (41%)	4/22 (18%)
RAVLT: interference	4.3 ± 2.3	12/22 (55%)	7/22 (32%)
RAVLT: delayed recall	6.3 ± 4.5	13/22 (59%)	13/22 (59%)
Attention			
TAP: alertness tonic	309.2 ± 71.6	15/22 (68%)	7/22 (32%)
TAP: alertness phasic	302.6 ± 72.1	15/21 (71%)	8/21 (38%)
TAP: divided attention visual	863.5 ± 141.0	3/20 (15%)	2/20 (10%)
TAP: divided attention auditory	590.8 ± 110.2	8/19 (42%)	3/19 (16%)
Executive functions			
Go/NoGo	600.5 ± 93.4	6/17 (35%)	2/17 (12%)
Working memory			
Digit span forward	7.0 ± 2.0	6/24 (25%)	4/24 (17%)
Digit span backward	6.0 ± 2.7	10/24 (42%)	5/24 (21%)

Abbreviations: No. = number; RAVLT = Rey Auditory Verbal Learning Test; ROCF = Rey–Osterrieth Complex Figure; TAP = Test Battery for Attention Performance.
Raw scores for attention and executive functions correspond to reaction times. Interpretation of test scores was based on patients' individual percentile ranks in comparison with age-specific norm values (see eMethods). Note that all patients with significant impairments (defined as scores ≤7th percentile of the norm, equivalent to ≈ −1.5 SD) also fulfilled the more liberal below-average criterion (defined as scores ≤16th percentile, equivalent to ≈ −1 SD). Therefore, all patients in the right column are also included in the middle column.

Figure 4B illustrates this approach for one participant whose individual brain topology closely adheres to the reference (*left panel*; low TDI; a control participant) and another one whose topology deviates strongly from the reference (*right panel*; high TDI; a patient with LGI1-E).

We then tested the difference in TDI values between HCs and patients with LGI1-E. Therein, we hypothesized that the HC group should show lower TDI values because (1) each healthy individual formed part of the group on which the reference was defined and (2) patients showed bidirectional alterations of BC in between-group testing. As expected, patients exhibited higher TDI values than HCs, with medium-to-large effect size ($t = 2.66$, $p = 0.011$, $d = 0.75$; Figure 4C). Subsequently, we related the TDI values of individual patients to their cognitive outcome scores in the domains of working memory, visuospatial memory, verbal episodic memory, executive function, and attention. While we observed no relationship between TDI and working memory ($r = −0.06$, 95% CI = [-0.45, 0.35], $p = 0.78$, n = 24, $p_{FDR} = 0.98$) or visuospatial memory ($r = 0.004$, CI = [−0.43 to 0.44], $p = 0.98$, n = 21, $p_{FDR} = 0.98$), higher topological deviation in patients was associated with reduced cognitive performance in the

domains of verbal episodic memory ($r = −0.56$, CI = [−0.79 to −0.18], $p = 0.007$, n = 22, $p_{FDR} = 0.017$), attention ($r = −0.55$, CI = [−0.79 to −0.16], $p = 0.008$, n = 22, $p_{FDR} = 0.017$), and executive functions ($r = −0.60$, CI = [−0.84 to −0.17], $p = 0.010$, n = 17, $p_{FDR} = 0.017$; Figure 4D).

Finally, exploratory follow-up analyses indicated that TDI values of patients were not significantly related to depression ($t = −0.11$, $p = 0.91$), arterial hypertension ($t = 0.38$, $p = 0.71$), or an interaction between them ($t = −0.63$, $p = 0.54$) at the time of MRI. Furthermore, there was no significant relationship between TDI and the time from disease onset ($\rho = −0.18$, $p = 0.39$). Moreover, patients who had received second-line immunotherapy did not differ from those with first-line therapy only—neither regarding TDI values ($t = 0.53$, $p = 0.60$) nor cognitive composite scores (all $p > 0.05$).

Discussion

This cross-sectional study combines diffusion-weighted neuroimaging, probabilistic tractography, computational methods, clinical evaluation, and neuropsychological assessments to characterize the relationship between WM networks and

Figure 2 White Matter Networks in Anti-LGI1 Encephalitis Are Characterized by Widespread Reductions in Structural Connectivity
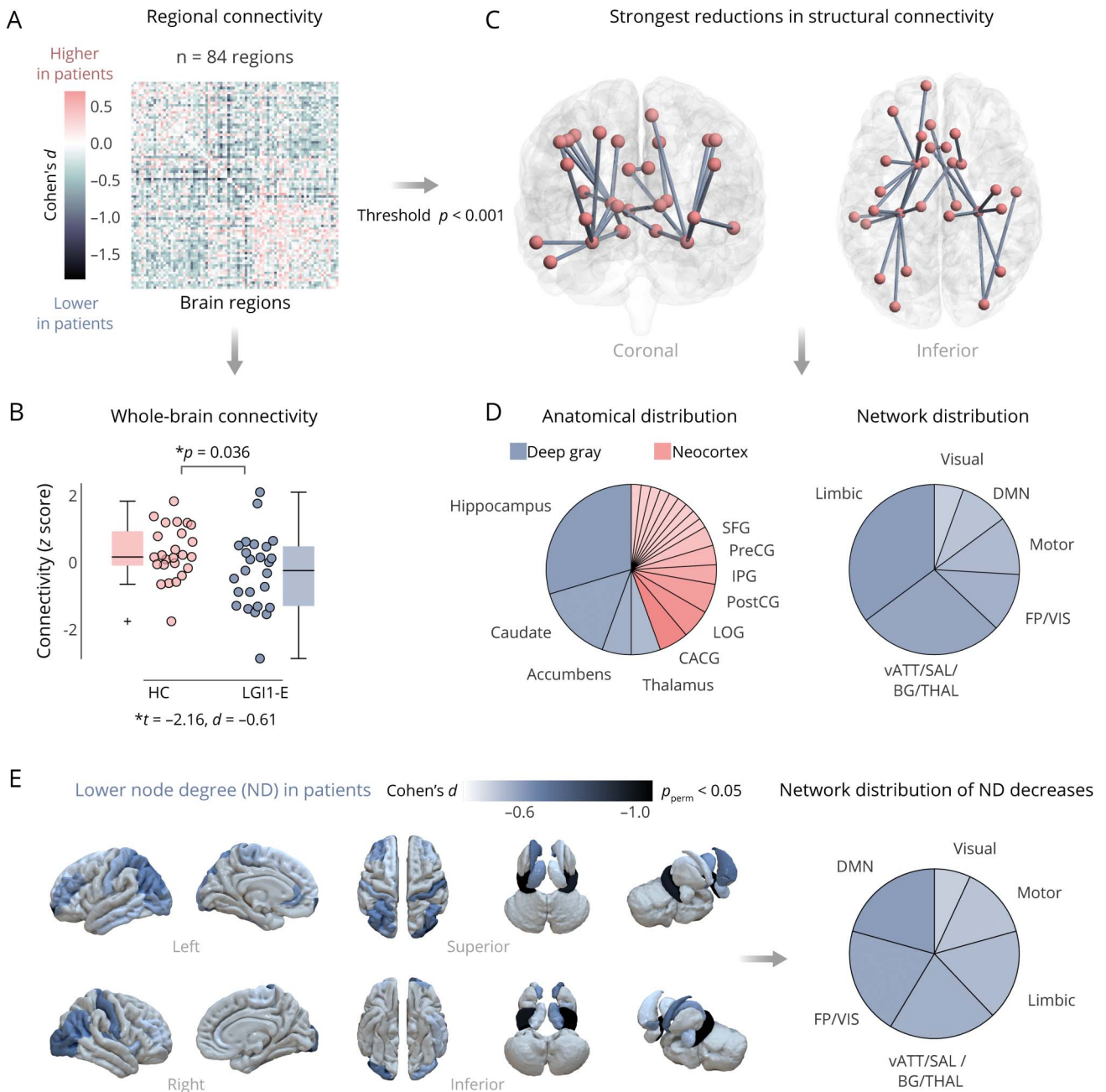
(A) Differences in structural connectivity strength between patients with anti-LGI1 encephalitis (LGI1-E) and healthy control (HC) participants across all 84 brain regions. The color bar represents the network-wide effect sizes of between-group comparisons (Cohen's d, n = 25 participants each). (B) Patients with LGI1-E show a reduction in whole-brain WM connectivity strength compared with HCs. (C) Network representation of region-wise connectivity differences from panel (A) in brain space. Group differences are thresholded to $p < 0.001$, at which only negative effects remain (i.e., reduced connectivity in LGI1-E). Nodes represent GM regions, and edges represent reduced SC of WM tracts between them. (D) Distribution of the connectivity reductions from panel (C) over anatomical structures (left) and functional network assignments (right). Anatomical labels correspond to the Desikan-Killiany atlas. For neocortical areas, gyri are abbreviated as follows: CACG = caudal anterior cingulate; IPG = inferior parietal; LOG = lateral occipital; postCG = postcentral; preCG = precentral; SFG = superior frontal gyrus. Cortical regions with only one entry are omitted for visibility and correspond to the following areas: superior temporal, middle temporal, inferior temporal, rostral anterior cingulate, paracentral, superior parietal, rostral middle frontal, caudal middle frontal, and frontal pole. Functional assignments rest on a novel region-to-network mapping procedure (see Methods). (E) Brain areas exhibiting decreased node degree (ND) in patients with LGI1-E. The color scale maps the effect size of the comparison with HCs given by Cohen's d (LGI1-E vs HC, n = 25 each; threshold: permuted $p < 0.05$). The right subpanel visualizes the distribution of brain areas with lower ND over functional systems. DMN = default mode network; FP/VIS = frontoparietal network/visual downstream; GM = gray matter; Limbic = mesolimbic network; Motor = somatomotor network; SC = structural connectivity; vATT/SAL/BG/THAL = ventral attention network/salience network/basal ganglia/thalamus; Visual = visual network; WM = white matter.

Figure 3 Patients With Anti-LGI1 Encephalitis Exhibit a Topological Reorganization of White Matter Networks
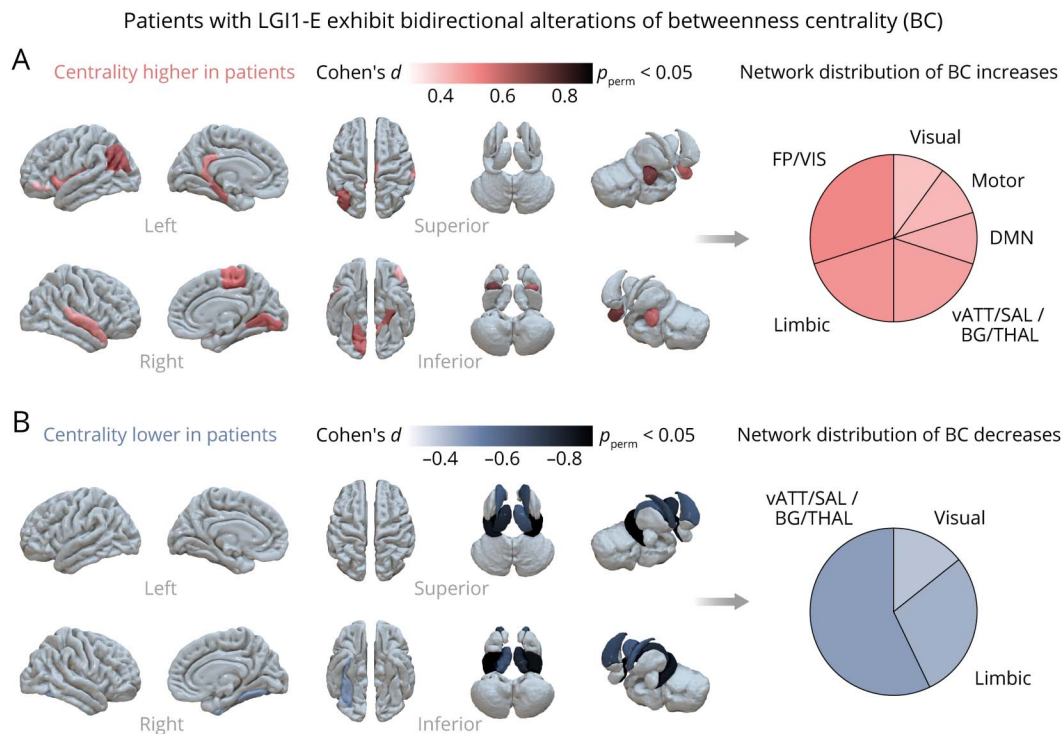
(A) Brain areas exhibiting increased betweenness centrality (BC) in patients with anti-LGI1 encephalitis (LGI1-E). The color scale maps the effect size of the comparison with healthy control (HC) participants, given by Cohen's d (LGI1-E vs HC, n = 25 each; threshold: permuted $p < 0.05$). BC increases primarily affect cortical areas and the amygdala bilaterally. The right panel visualizes the distribution of BC increases over functional systems. (B) Brain areas exhibiting decreased BC in patients with LGI1-E. BC decreases primarily affect the basal ganglia, the thalamus, and the hippocampus bilaterally. The color scale maps the effect size of the between-group comparison, and the right panel visualizes the network distribution of BC decreases. Functional assignments rest on region-to-network mapping (see Methods). DMN = default mode network; FP/VIS = frontoparietal network/visual downstream; Limbic = mesolimbic network; Motor = somatomotor network; vATT/SAL/BG/THAL = ventral attention network/salience network/basal ganglia/thalamus; Visual = visual network.

cognitive outcomes in patients with LGI1-E. Specifically, we show that (1) LGI1-E is characterized by SC reductions that cluster in limbic areas—as expected—but additionally affect an unexpectedly wide range of extralimbic brain systems, (2) WM networks in LGI1-E undergo a "topological re-organization" marked by a bidirectional shift in the relative importance of individual brain regions in the network, (3) patients with LGI1-E show persistent cognitive deficits despite immunotherapy and good overall clinical recovery, (4) these deficits affect multiple cognitive domains beyond memory dysfunction, and (5) this multidomain cognitive impairment is strongly linked to the structural reorganization of WM networks in the postacute disease stage. Collectively, these findings advance our understanding of LGI1-E along three principal directions.

First, it has become increasingly clear that cognitive deficits represent a key clinical outcome of LGI1-E.[6,8,15,16,38,39] Specifically, recent evidence suggests that cognitive impairment in LGI1-E is not limited to memory deficits,[8] which are frequently observed in limbic encephalitis due to affliction of the MTL. Instead, patients with LGI1-E commonly show *multidomain* deficits beyond memory impairment,[16-18] involving executive functions, language skills, psychomotor speed, and attentional

capacities—cognitive domains not classically attributed to the limbic system. Our study clearly strengthens this view by showing that WM changes are not only linked to reduced performance in the domain of verbal memory but also relate to persistent deficits in executive functions and attention.

Furthermore, there is accumulating evidence that cognitive deficits in LGI1-E persist well into the postacute disease phase. Although up to 80% of patients show fast responses to immunotherapy regarding seizures, cognitive recovery is much more protracted, with most patients reporting residual cognitive deficits after ≥2 years.[5] It is important to note that even with immunotherapy, only approximately 35% of patients with LGI1-E return to their baseline cognitive function, and at least 20% of patients require assistance in daily living because of persistent cognitive deficits.[40] Strikingly, although all our patients had received immunotherapy at peak illness, we found that cognitive symptoms strongly persisted into the postacute phase—in spite of good overall improvement on the mRS and the more disease-specific CASE score.[22] These findings converge well with recent related reports on long-term outcomes in LGI1-E, which similarly observed substantial residual symptoms across cognition and fatigue.[15,38] As such, although patients may show good recovery regarding

Figure 4 The Extent of White Matter Reorganization Is Associated With Multidomain Cognitive Impairment in Patients With Anti-LGI1 Encephalitis
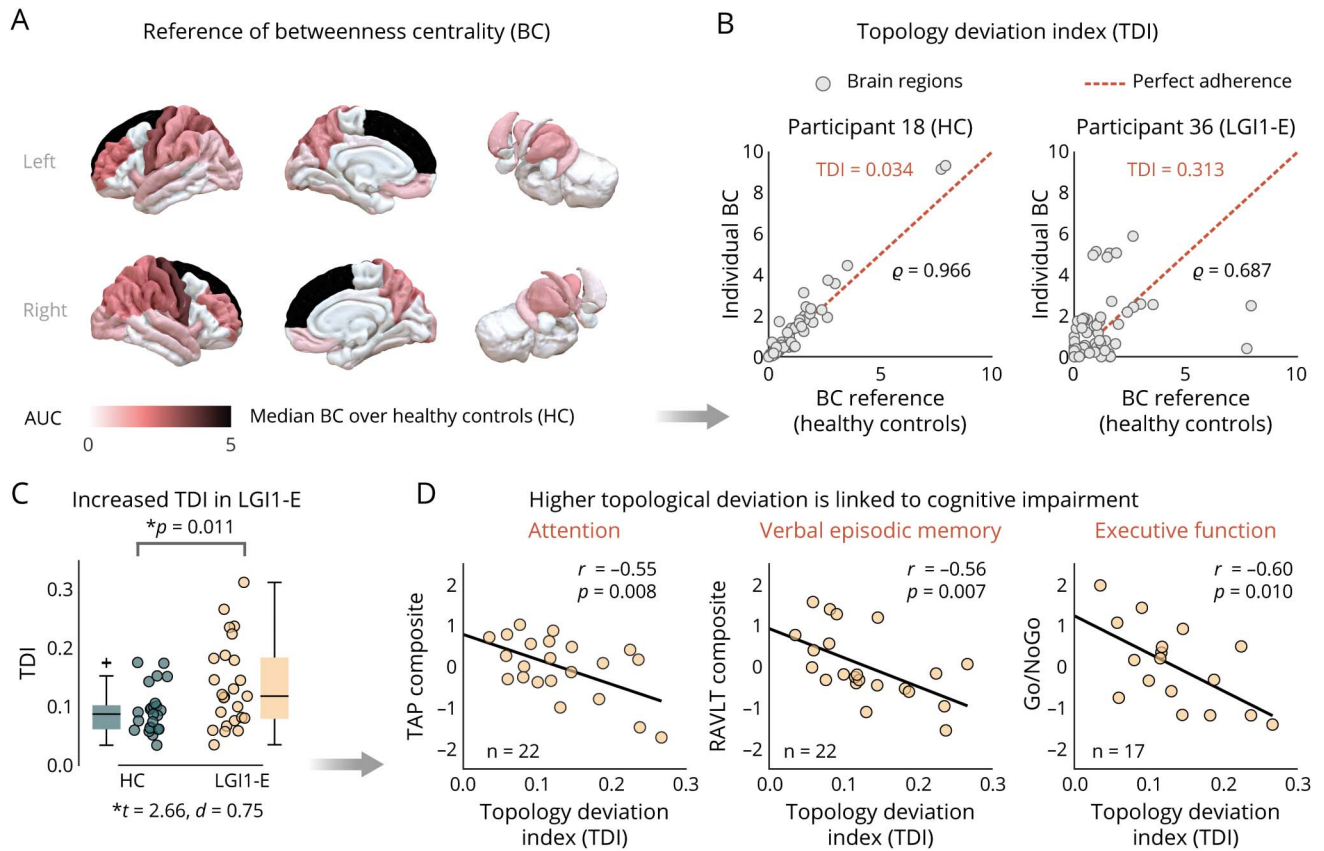
(A) Reference distribution of betweenness centrality (BC), computed as the median BC value across all 25 healthy control (HC) participants for every brain region. (B) Illustration of the topology deviation index (TDI), computed as the nonparametric correlation distance between the BC distribution of an individual participant (y-axis) and the reference distribution from panel (A) (x-axis). The left plot illustrates a control participant with low topological deviation and the right plot a patient with high deviation. (C) Patients with anti-LGI1 encephalitis show higher TDI scores than HCs (t test, n = 25 each group, d: effect size). (D) Higher TDI scores in patients are associated with impaired cognitive performance across multiple cognitive domains (all $p_{FDR} < 0.02$).

mRS or CASE scores, it has been argued that these improvements are not "good enough,"[41] given that at least two-thirds of patients suffer from residual deficits of cognition, mood, or fatigue and only approximately 15% are able to return to work.[1,38] Notably, these return rates in LGI1-E are substantially lower compared with anti-NMDA receptor encephalitis, in which 65%–70% of patients return to work or school,[42] highlighting disease-specific differences in long-term outcomes. Not least, recent evidence also shows that residual cognitive dysfunction after the initial episode of LGI1-E is associated with an increased risk of relapse, which occurs in 15%–25% of patients.[43]

In consequence, a crucial open question is how these residual cognitive deficits in LGI1-E relate to long-term changes in brain structure. Our study identifies such a link by showing that cognitive performance in the postacute stage is more impaired in patients whose brains exhibit a higher degree of structural reorganization. Notably, this relationship was not confined to focal brain regions but rather features many simultaneous changes across the global WM network.

A second open question concerns the spatial pattern of brain damage in LGI1-E. In line with previous studies,[8,44] we observed strong alterations in limbic brain structures, and specifically the hippocampus, which showed a clear reduction in raw WM connectivity, ND (a graph measure of overall connectedness), and BC (a measure of relative importance in the network). Crucially, however, our novel region-to-network mapping procedure revealed that LGI1-E additionally involves widespread alterations of extralimbic brain systems, including not only the basal ganglia, amygdalae, and thalamus but also higher order cognitive systems such as the default mode network and salience areas. Although LGI1-E is traditionally conceptualized as a form of "limbic" encephalitis,[7] these findings suggest that it should rather be understood as a global "network disorder"—a view that may help reconcile diverse previous findings on clinical course and neuroimaging changes: specifically, our findings align remarkably well with the widespread disruption of functional brain networks in LGI1-E,[10] suggesting that these changes in brain activity are a direct expression of alterations in the WM tracts connecting spatially distant GM regions. Similarly, a recent study has

suggested that memory impairment in AE may not be entirely explained by hippocampal dysfunction alone but rather by wider network alterations involving the cingulate, thalamus, precuneus, prefrontal cortex, and posteromedial cortex.[45] Because abnormalities in clinical MRI are typically strongest in the MTL,[5,9] where LGI1 expression clusters,[46] it has been hypothesized that such a disruption across the wider network may develop secondary to focal hippocampal damage and may not be directly caused by autoantibody-mediated mechanisms.[11]

In this context, a network view of LGI1-E also aligns well with the temporal dynamics of clinical manifestation, which typically involves a primary, often seizure-dominant symptom complex at onset and subsequently progresses to include additional features such as psychiatric symptoms and cognitive deficits with a latency of weeks to months.[47] In consequence, the long-term alterations of WM networks observed here suggest that LGI1-E may primarily cause focal brain damage initially and only subsequently affect other regions through their structural connections to this initial target—a process compatible with the mechanistic idea of "connectomal diaschisis"[48] that could explain both the latency and persistence of cognitive deficits.

Third, the high prevalence of residual symptoms despite immunotherapy has prompted the argument that LGI1-E and other forms of AE should be viewed as only partially immunotherapy-responsive conditions for which significant advances in clinical management are necessary to improve long-term outcomes.[1] Consequently, objective markers that guide postacute treatment are urgently needed because cognitive deficits are a key contributor to long-term disability,[8,15,16] and every fifth patient with LGI1-E lives in dependency.[49] Our study presents the TDI as a novel neuroimaging marker that was highly sensitive to cognitive impairment in the postacute disease stage and represents a promising new outcome measure for prospective clinical trials. Furthermore, our approach explicitly captures patient-specific patterns of brain alterations because the TDI is agnostic to which particular regions show the strongest deviations from the reference group,[36] yielding a highly personalized outcome marker. Not least, this comparison of individual MRI scans with a healthy reference population represents the first step toward a normative neuroimaging framework—similar to diagnostic laboratory tests in which the patient's score is compared with a reference range—and may thus serve as a biomarker to monitor disease course and treatment response.

Limitations of our study include the cross-sectional design, which precludes inferences about the onset of WM reorganization in LGI1-E and whether it is reversible. In this context, our study clearly shows that neither these network changes nor the associated cognitive deficits were prevented by the applied immunotherapy. Therefore, our results call for future trials to evaluate whether patients benefit from closer postacute monitoring and whether more aggressive or sustained immunotherapy is able to modify this long-term

disease course. Similarly, patients in our study were included ad hoc on referral to our reference center, resulting in variable intervals since the acute disease phase. While we did not observe a significant association between WM changes and time since disease onset, future longitudinal studies are needed to describe the temporal trajectories of WM reorganization in LGI1-E systematically.

Moreover, the role of comorbidities regarding WM changes warrants further study. While we did not observe an effect of depression or arterial hypertension on WM reorganization here, diagnostic data on these factors were binary and extracted retrospectively. Therefore, future studies are needed to characterize comorbidities prospectively, including a more comprehensive account of cardiovascular risk profiles. Furthermore, while the normative neuroimaging approach developed here proved highly sensitive in our sample, the healthy reference population was rather small. Consequently, future work in larger samples is needed to characterize the interindividual variability of WM networks in healthy participants and to derive age-specific and sex-specific normative values.

Finally, while it is now clear that cognitive deficits represent a key outcome of LGI1-E, cognitive impairment shows a complex interrelationship with fatigue, which has recently been shown to affect patient-reported quality of life in the postacute stage.[50] Therefore, a natural next step will be to assess how WM reorganization relates to persistent fatigue.

In conclusion, although LGI1-E is traditionally viewed as a form of "limbic" encephalitis, our study characterizes it as a global "network disorder" that affects both limbic and extralimbic brain systems. Moreover, we find that a reorganization of WM networks is linked to persistent and multidomain cognitive impairment in the postacute disease stage—despite immunotherapy and good overall recovery. These findings highlight the need for better monitoring and improved treatment strategies to mitigate long-term cognitive impairment and propose a sensitive new neuroimaging marker for future clinical trials.

Author Contributions

S. Krohn: drafting/revision of the manuscript for content, including medical writing for content; major role in the acquisition of data; study concept or design; analysis or interpretation of data. L. Müller-Jensen: drafting/revision of the manuscript for content, including medical writing for content; major role in the acquisition of data; study concept or design; analysis or interpretation of data. J. Kuchling: drafting/revision of the manuscript for content, including medical writing for content; analysis or interpretation of data. A. Romanello: drafting/revision of the manuscript for content, including medical writing for content; analysis or interpretation of data. K. Wurdack: drafting/revision of the manuscript for content, including medical writing for content; major role in the acquisition of data. S. Rekers: drafting/

Study Funding

Disclosure

Publication History

References

1. Varley JA, Strippel C, Handel A, Irani SR. Autoimmune encephalitis: recent clinical and biological advances. *J Neurol* 2023;270(8):4118-4131. doi:10.1007/s00415-023-11685-3
2. Lai M, Huijbers MG, Lancaster E, et al. Investigation of LGI1 as the antigen in limbic encephalitis previously attributed to potassium channels: a case series. *Lancet Neurol* 2010;9(8):776-785. doi:10.1016/S1474-4422(10)70137-X
3. Irani SR, Michell AW, Lang B, et al. Faciobrachial dystonic seizures precede LGI1 antibody limbic encephalitis. *Ann Neurol.* 2011;69(5):892-900. doi:10.1002/ana.22307
4. Irani SR, Alexander S, Waters P, et al. Antibodies to Kv1 potassium channel-complex proteins leucine-rich, glioma inactivated 1 protein and contactin-associated protein-2 in limbic encephalitis, Morvan's syndrome and acquired neuromyotonia. *Brain.* 2010; 133(9):2734-2748. doi:10.1093/brain/awq213
5. van Sonderen A, Thijs RD, Coenders EC, et al. Anti-LGI1 encephalitis: clinical syndrome and long-term follow-up. *Neurology.* 2016;87(14):1449-1456. doi:10.1212/WNL.0000000000003173
6. Muñoz-Lopetegi A, Guasp M, Prades L, et al. Neurological, psychiatric, and sleep investigations after treatment of anti-leucine-rich glioma-inactivated protein 1 (LGI1) encephalitis in Spain: a prospective cohort study. *Lancet Neurol.* 2024;23(3):256-266. doi:10.1016/S1474-4422(23)00463-5
7. Tüzün E, Dalmau J. Limbic encephalitis and variants: classification, diagnosis and treatment. *Neurologist.* 2007;13(5):261-271. doi:10.1097/NRL.0b013e31813e34a5
8. Finke C, Prüss H, Heine J, et al. Evaluation of cognitive deficits and structural hippocampal damage in encephalitis with leucine-rich, glioma-inactivated 1 antibodies. *JAMA Neurol.* 2017;74(1):50-59. doi:10.1001/jamaneurol.2016.4226

9. Kelly MJ, Grant E, Murchison AG, et al. Magnetic resonance imaging characteristics of LGI1-antibody and CASPR2-antibody encephalitis. *JAMA Neurol*. 2024;81(5):525-533. doi:10.1001/jamaneurol.2024.0126

10. Heine J, Prüss H, Kopp UA, et al. Beyond the limbic system: disruption and functional compensation of large-scale brain networks in patients with anti-LGI1 encephalitis. *J Neurol Neurosurg Psychiatry*. 2018;89(11):1191-1199. doi:10.1136/jnnp-2017-317780

11. Loane C, Argyropoulos GPD, Roca-Fernández A, et al. Hippocampal network abnormalities explain amnesia after VGKCC-Ab related autoimmune limbic encephalitis. *J Neurol Neurosurg Psychiatry* 2019;90(9):965-974. doi:10.1136/jnnp-2018-320168

12. Rissanen E, Carter K, Cicero S, et al. Cortical and subcortical dysmetabolism are dynamic markers of clinical disability and course in anti-LGI1 encephalitis. *Neurol Neuroimmunol Neuroinflamm*. 2022;9(2):e1136. doi:10.1212/NXI.0000000000001136

13. Navarro V, Kas A, Apartis E, et al. Motor cortex and hippocampus are the two main cortical targets in LGI1-antibody encephalitis. *Brain*. 2016;139(Pt 4):1079-1093. doi:10.1093/brain/aww012

14. Qiao J, Zhao X, Wang S, et al. Functional and structural brain alterations in encephalitis with LGI1 antibodies. *Front Neurosci*. 2020;14:304. doi:10.3389/fnins.2020.00304

15. Aboseif A, Li Y, Amin M, et al. Clinical determinants of longitudinal disability in LGI-1-IgG autoimmune encephalitis. *Neurol Neuroimmunol Neuroinflamm*. 2024;11(1):e200178. doi:10.1212/NXI.0000000000200178

16. Galioto R, Aboseif A, Krishnan K, Lace J, Kunchok A. Cognitive outcomes in anti-LGI-1 encephalitis. *J Int Neuropsychol Soc*. 2023;29(6):541-550. doi:10.1017/S1355617722000509

17. Galioto R, Grezmak T, Swetlik C, et al. Neuropsychological testing in autoimmune encephalitis: a scoping review. *Neurol Neuroimmunol Neuroinflamm*. 2024;11(1):e200179. doi:10.1212/NXI.0000000000200179

18. Bettcher BM, Gelfand JM, Irani SR, et al. More than memory impairment in voltage-gated potassium channel complex encephalopathy. *Euro J Neurol*. 2014;21(10):1301-1310. doi:10.1111/ene.12482

19. Smith RE, Raffelt D, Tournierc JD, Connelly A. Quantitative streamlines tractography: methods and inter-subject normalisation. *Aperture Neuro*. 2022:1-25. doi:10.52294/ApertureNeuro.2022.2.NEOD9565

20. Bullmore E, Sporns O. Complex brain networks: graph theoretical analysis of structural and functional systems. *Nat Rev Neurosci*. 2009;10(3):186-198. doi:10.1038/nrn2575

21. Graus F, Titulaer MJ, Balu R, et al. A clinical approach to diagnosis of autoimmune encephalitis. *Lancet Neurol*. 2016;15(4):391-404. doi:10.1016/S1474-4422(15)00401-9

22. Lim JA, Lee ST, Moon J, et al. Development of the clinical assessment scale in autoimmune encephalitis: development of the CASE. *Ann Neurol*. 2019;85(3):352-358. doi:10.1002/ana.25421

23. Ho DE, Imai K, King G, Stuart EA. MatchIt: nonparametric preprocessing for parametric causal inference. *J Stat Soft*. 2011;42(8). doi:10.18637/jss.v042.i08

24. Tournier JD, Smith R, Raffelt D, et al. MRtrix3: a fast, flexible and open software framework for medical image processing and visualisation. *Neuroimage*. 2019;202:116137. doi:10.1016/j.neuroimage.2019.116137

25. Jenkinson M, Beckmann CF, Behrens TEJ, Woolrich MW, Smith SM. FSL. *Neuroimage*. 2012;62(2):782-790. doi:10.1016/j.neuroimage.2011.09.015

26. Avants B, Tustison NJ, Song G. Advanced normalization tools: V1.0. *Insight J*. 2009. doi:10.54294/uvnhin

27. Smith RE, Tournier JD, Calamante F, Connelly A. Anatomically-constrained tractography: improved diffusion MRI streamlines tractography through effective use of anatomical information. *NeuroImage* 2012;62(3):1924-1938. doi:10.1016/j.neuroimage.2012.06.005

28. Desikan RS, Ségonne F, Fischl B, et al. An automated labeling system for subdividing the human cerebral cortex on MRI scans into gyral based regions of interest. *Neuroimage*. 2006;31(3):968-980. doi:10.1016/j.neuroimage.2006.01.021

29. Zhang Y, Brady M, Smith S. Segmentation of brain MR images through a hidden Markov random field model and the expectation-maximization algorithm. *IEEE Trans Med Imaging*. 2001;20(1):45-57. doi:10.1109/42.906424

30. Smith RE, Tournier JD, Calamante F, Connelly A. SIFT2: enabling dense quantitative assessment of brain white matter connectivity using streamlines tractography. *Neuroimage*. 2015;119:338-351. doi:10.1016/j.neuroimage.2015.06.092

31. Hechler A, Kuchling J, Müller-Jensen L, et al. Hippocampal hub failure is linked to long-term memory impairment in anti-NMDA-receptor encephalitis: insights from structural connectome graph theoretical network analysis. *J Neurol*. 2024;271(9):5886-5898. doi:10.1007/s00415-024-12545-4

32. Urchs S, Armoza J, Moreau C, et al. MIST: a multi-resolution parcellation of functional brain networks. *MNI Open Res*. 2019;1:3. doi:10.12688/mniopenres.12767.2

33. Sporns O, Tononi G, Kötter R. The human connectome: a structural description of the human brain. *Plos Comp Biol*. 2005;1(4):e42. doi:10.1371/journal.pcbi.0010042

34. Rubinov M, Sporns O. Complex network measures of brain connectivity: uses and interpretations. *Neuroimage*. 2010;52(3):1059-1069. doi:10.1016/j.neuroimage.2009.10.003

35. Bullmore E, Sporns O. The economy of brain network organization. *Nat Rev Neurosci*. 2012;13(5):336-349. doi:10.1038/nrn3214

36. Krohn S, von Schwanenflug N, Romanello A, Valk SL, Madan CR, Finke C. The formation of brain shape in human newborns. *bioRxiv (neuroscience)*. 2023. doi:10.1101/2023.01.01.521756

37. Benjamini Y, Hochberg Y. Controlling the false discovery rate: a practical and powerful approach to multiple testing. *J R Stat Soc Ser B Stat Methodol*. 1995;57(1):289-300. doi:10.1111/j.2517-6161.1995.tb02031.x

38. Binks SNM, Veldsman M, Easton A, et al. Residual fatigue and cognitive deficits in patients after leucine-rich glioma-inactivated 1 antibody encephalitis. *JAMA Neurol*. 2021;78(5):617-619. doi:10.1001/jamaneurol.2021.0477

39. Rodriguez A, Klein CJ, Sechi E, et al. LGI1 antibody encephalitis: acute treatment comparisons and outcome. *J Neurol Neurosurg Psychiatry*. 2022;93(3):309-315. doi:10.1136/jnnp-2021-327302

40. Ariño H, Armangué T, Petit-Pedrol M, et al. Anti-LGI1–associated cognitive impairment: presentation and long-term outcome. *Neurology*. 2016;87(8):759-765. doi:10.1212/WNL.0000000000003009

41. Day GS. Rethinking outcomes in leucine-rich, glioma-inactivated 1 protein encephalitis: "good" isn't good enough. *JAMA Neurol*. 2017;74(1):19-21. doi:10.1001/jamaneurol.2016.4538

42. Blum RA, Tomlinson AR, Jetté N, Kwon CS, Easton A, Yeshokumar AK. Assessment of long-term psychosocial outcomes in anti-NMDA receptor encephalitis. *Epilepsy Behav*. 2020;108:107088. doi:10.1016/j.yebeh.2020.107088

43. Campetella L, Farina A, Villagrán-García M, et al. Predictors and clinical characteristics of relapses in LGI1-antibody encephalitis. *Neurol Neuroimmunol Neuroinflamm*. 2024;11(3):e200228. doi:10.1212/NXI.0000000000200228

44. Miller TD, Chong TTJ, Aimola Davies AM, et al. Focal CA3 hippocampal subfield atrophy following LGI1 VGKC-complex antibody limbic encephalitis. *Brain*. 2017;140(5):1212-1219. doi:10.1093/brain/awx070

45. Argyropoulos GP, Loane C, Roca-Fernandez A, et al. Network-wide abnormalities explain memory variability in hippocampal amnesia. *eLife*. 2019;8:e46156. doi:10.7554/eLife.46156

46. Herranz-Pérez V, Olucha-Bordonau FE, Morante-Redolat JM, Pérez-Tur J. Regional distribution of the leucine-rich glioma inactivated (LGI) gene family transcripts in the adult mouse brain. *Brain Res*. 2010;1307:177-194. doi:10.1016/j.brainres.2009.10.013

47. Thompson J, Bi M, Murchison AG, et al. The importance of early immunotherapy in patients with faciobrachial dystonic seizures. *Brain*. 2018;141(2):348-356. doi:10.1093/brain/awx323

48. Carrera E, Tononi G. Diaschisis: past, present, future. *Brain*. 2014;137(Pt 9):2408-2422. doi:10.1093/brain/awu101

49. Thaler FS, Zimmermann L, Kammermeier S, et al. Rituximab treatment and long-term outcome of patients with autoimmune encephalitis: real-world evidence from the GENERATE registry. *Neurol Neuroimmunol Neuroinflamm*. 2021;8(6):e1088. doi:10.1212/NXI.0000000000001088

50. Binks SNM, Veldsman M, Handel AE, et al. Fatigue predicts quality of life after leucine-rich glioma-inactivated 1-antibody encephalitis. *Ann Clin Transl Neurol*. 2024;11(4):1053-1058. doi:10.1002/acn3.52006